

Article

Synergistic Effect of La and TiB₂ Particles on Grain Refinement in Aluminum Alloy

Lili Zhang ^{1,*}, Yan Song ^{1,2,†}, Linjie Yang ^{1,2}, Jiuzhou Zhao ^{1,2,*}, Jie He ^{1,2} and Hongxiang Jiang ^{1,2}

¹ Shi-Changxu Innovation Centre for Advanced Materials, Institute of Metal Research, Chinese Academy of Sciences, Shenyang 110016, China; ysong16b@imr.ac.cn (Y.S.); ljiang19s@imr.ac.cn (L.Y.); jhe@imr.ac.cn (J.H.); hxjiang@imr.ac.cn (H.J.)

² School of Materials Science and Engineering, University of Science and Technology of China, Shenyang 110016, China

* Correspondence: llzhang@imr.ac.cn (L.Z.); jzzhao@imr.ac.cn (J.Z.)

† These authors contributed equally to this work.

Abstract: Synergistic effect of TiB₂ (in form of Al-5Ti-1B) and La on grain refining results in Al-2Cu alloy was investigated. α -Al grains are significantly refined by Al-5Ti-1B. When trace La is added to the melt, further refinement is exhibited. Average grain size and nucleation undercooling of α -Al reduce first and then almost remain unchanged with La addition. Satisfactory grain refining result achieves when La addition level reaches 600 ppm. When more than 600 ppm La is added to the melt, La-rich particles form and the effect of solute La left in matrix on the microstructure almost no longer changes. Theoretical calculation results demonstrate that solute La segregates to Al melt/TiB₂ particles interface along with Ti and Cu prior to α -Al nucleation and the synergistic effect of La and TiB₂ particles on grain refinement mainly attributes to the enhancement in the potency of TiB₂ particles to heterogeneously nucleate α -Al by trace La addition.

Keywords: grain refinement; microstructure; segregation; heterogeneous nucleation; metals and alloys



Citation: Zhang, L.; Song, Y.; Yang, L.; Zhao, J.; He, J.; Jiang, H. Synergistic Effect of La and TiB₂ Particles on Grain Refinement in Aluminum Alloy. *Materials* **2022**, *15*, 0. <https://doi.org/>

Academic Editor: Filippo Berto

Received: 10 December 2021

Accepted: 26 December 2021

Published: 29 December 2021

Publisher's Note: MDPI stays neutral with regard to jurisdictional claims in published maps and institutional affiliations.



Copyright: © 2021 by the authors. Licensee MDPI, Basel, Switzerland. This article is an open access article distributed under the terms and conditions of the Creative Commons Attribution (CC BY) license (<https://creativecommons.org/licenses/by/4.0/>).

1. Introduction

Grain refinement contributes to the enhancement in mechanical properties of alloys. Inoculation by adding master alloys (such as Al-Zr, Al-Cr, Al-B, and Al-Ti-B) to melt has been widely employed to improve the microstructures of aluminum alloys [1–3]. Among them, Al-5Ti-1B (mass percent, the same as below unless otherwise specified) master alloy is the most widely used grain refiner. Since the introduction of Al-Ti-B, much work has been done to explore microstructure formation in aluminum alloys under the effect of grain refiners [4–13]. It is now acknowledged that size distribution of TiB₂ and solute Ti concentration play an important role in grain refinement.

TiB₂ particles heterogeneously nucleate α -Al grains, while solute Ti affects the potency of TiB₂ to heterogeneously nucleate α -Al and restricts growth of α -Al grains, which is quantitatively described as growth restriction factor $Q_{Ti} (= m_{Ti}c_{Ti}^0(k_{Ti} - 1))$, c_{Ti}^0 , $k_{Ti} = 7.8$, and $m_{Ti} = 33.3$ K/wt% are respectively the solute Ti concentration, equilibrium partition coefficient, and liquidus slope in Al-Ti phase diagram [9]. When solute Ti concentration is low, contact angle between α -Al and TiB₂ particles is large and restriction effect of solute Ti on α -Al growth is small. This results in a weak grain refinement result and only columnar grain structure is refined. Grain refinement result enhances and columnar-to-equiaxed transition is present when solute Ti concentration is high.

In spite of great progress in the investigation of microstructure formation in inoculated aluminum alloys, limited grain refinement potency of Al-5Ti-1B cannot meet the requirement for manufacturing high-quality aluminum alloys. Enhancement in grain refinement of Al-5Ti-1B is quite necessary in industry. La, one of the most economical rare elements, has attracted much attention since the 1990s due to its significant effect on grain refinement

of matrix [14,15] and modification of phases in aluminum alloys [14,16–18]. Recently, attention is shifting to the synergistic effect of La and other elements, such as B [19], Mg [20], and Sr [21], on microstructures of aluminum alloys. Our latest work demonstrates that only a few hundred ppm of La is enough to improve the microstructures [22–24]. Considering the wide use of Al-5Ti-1B and great potentials of La in improving microstructure, it is necessary to explore the combined effect of TiB₂ particles and trace La on microstructure evolution of aluminum alloys.

2. Materials and Methods

High-purity Al (99.99%), Cu (99.999%), and La (99.99%) and Al-5Ti-1B prepared in our lab were used as raw materials. Al-2Cu and Al-10La alloys are respectively prepared as follows: first, melting high-purity Al and heating to 1003 K; then, adding high-purity Cu or La to melt and holding the melt at 1003 K for 30 min; finally, solidifying the melt to obtain Al-2Cu and Al-10La alloys. The process for grain refinement was as follows: first, melting Al-2Cu alloy and heating to 1003 K; then, adding trace La to melt in form of Al-10La and holding the melt at 1003 K for 20 min; after that, adding Al-5Ti-1B to melt and holding the melt at 1003 K for 10 min; finally, solidifying the melt to form an ingot with a diameter of 20 mm and height of 40 mm. Temperature at the center of cross-section approximately 15 mm from bottom was measured using tungsten–rhenium thermocouple of 0.2 mm in radius. The cooling rate of the melt is about 20 K/s.

Process described in reference [23] was employed to prepare metallographic specimens. Microstructures of α -Al were examined by using Zeiss optical microscope (Carl Zeiss AG, Germany) with polarized light after the specimens were ground, polished electrolytically for about 20 s at 50 V in a reagent (5 vol% HClO₄ in ethanol solution) and anodized for about 120 s at 20 V in Barker's reagent (2.5 vol% HBF₄ in distilled water). Sizes of α -Al grains, obtained from the same center region of the cross-section, were determined by quantitative metallographic analysis using SISC IAS V8.0 software. Scanning electron microscopy (SEM, Quanta 450, FEI, Hillsboro, FL, USA) equipped with an energy dispersive X-ray spectroscopy (EDS) was also used to characterize the microstructure. Differential thermal analyzer (DTA, Beijing Jingyi gaoke Instrument Co., Ltd., Beijing, China) experiments were performed with heating/cooling rate of 10 K/min. Transmission electron microscope (TEM) is also employed to characterize microstructures. Specimens for TEM investigation were first cut into discs with a diameter of 3 mm and thickness of 0.5 mm and ground to a thickness of about 50 μ m. Discs were then dimpled and ion-beam-thinned by using Gatan Precision Ion Polishing System (Gatan 691, Gatan, Pleasanton, CA, USA) under the conditions of 1–5 kV and an incident angle of 3–8°. TEM analyses were performed by using Tecnai G2 20 (FEI, Hillsboro, FL, USA).

3. Results

Figures 1 and 2 respectively show microstructures and average grain sizes of Al-2Cu alloy without addition of inoculant and by adding 0.4% Al-5Ti-1B + trace La. α -Al grains are significantly refined by 0.4% Al-5Ti-1B with the average grain size of α -Al decreasing to $187 \pm 5 \mu$ m from $654 \pm 4 \mu$ m. Microstructure exhibits a further refinement when La is introduced and grain size decreases first and then almost keeps unchanged with La addition.

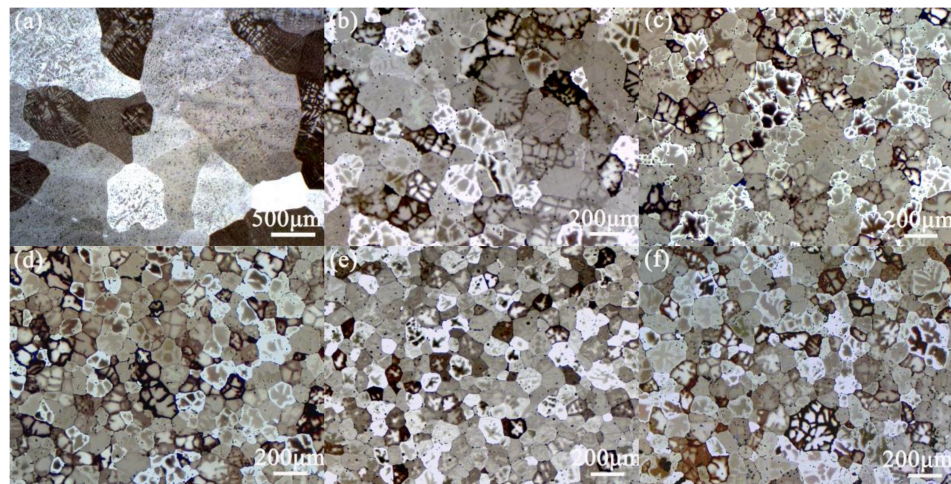


Figure 1. Microstructures of Al-2Cu alloy (a) without addition of inoculant and by adding 0.4% Al-5Ti-1B + La addition of (b) 0%, (c) 0.02%, (d) 0.06%, (e) 0.08%, and (f) 0.10%.

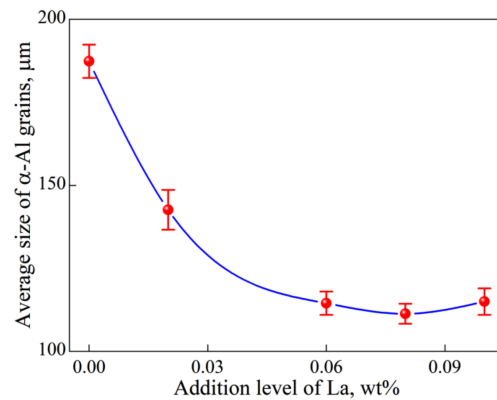


Figure 2. Average size of α -Al grains in Al-2Cu alloy by adding 0.4% Al-5Ti-1B vs. La addition level.

Figure 3 shows the SEM image and EDS line-scanning results for Al-2Cu alloy inoculated with 0.4% Al-5Ti-1B + 0.08% La. The results demonstrate that trace La enriches at the surface of TiB_2 particles along with solutes Cu and Ti.

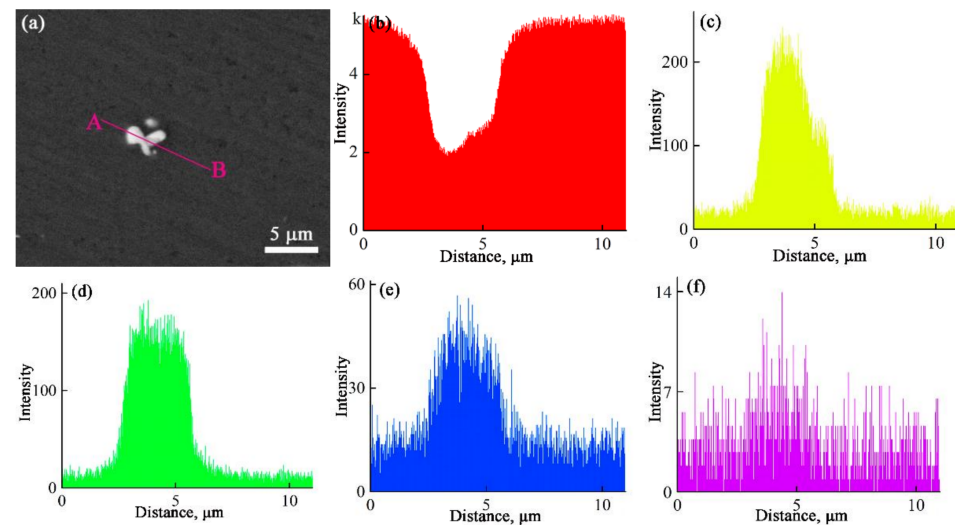


Figure 3. SEM image and EDS line-scanning results for Al-2Cu alloy inoculated with 0.4% Al-5Ti-1B + 0.08% La. (a) back-scattered electron image; (b–f) distributions of Al, Cu, La, Ti, and B along line A and B.

TEM elemental map results demonstrate that La-rich particles ($\text{Al}_6\text{Cu}_6\text{La}$) form when La addition reaches 0.08%, as shown in Figure 4.

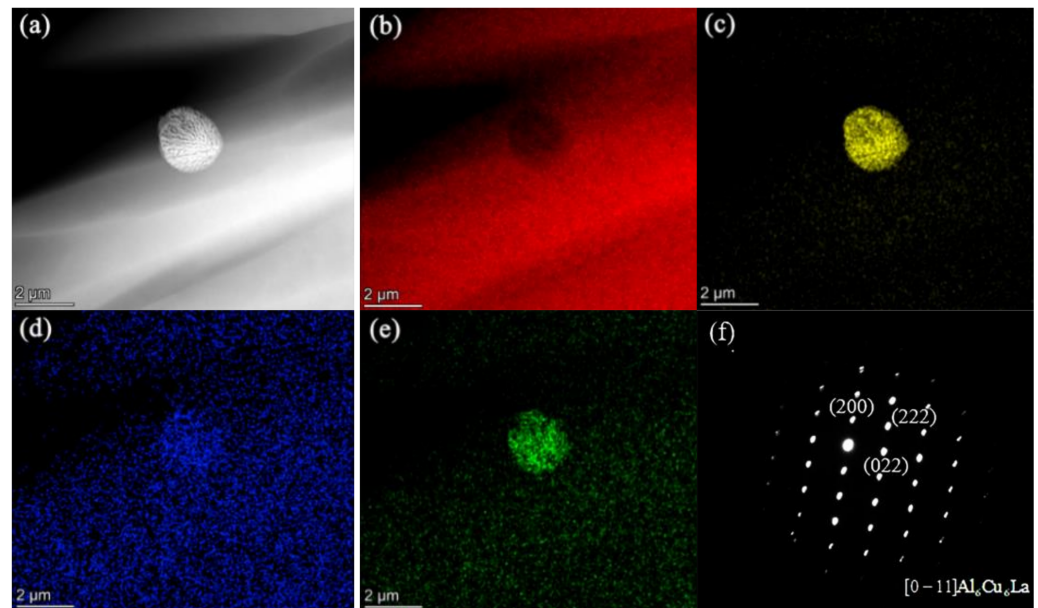


Figure 4. (a) TEM image, elemental maps of (b) Al, (c) Cu, (d) Ti, and (e) La and (f) selected area electron diffraction pattern in the zone axis of $[0-11]\text{Al}_6\text{Cu}_6\text{La}$ of the particles consisted of Al, Cu, and La in Al-2Cu alloy by adding 0.4% Al-5Ti-1B + 0.08% La.

Figure 5 shows DTA curves of Al-2Cu alloy by adding 0.4% Al-5Ti-1B + trace La. Onset temperatures of exothermic and endothermic peaks are respectively the nucleation temperature T_n and melting temperature T_m of α -Al. The nucleation undercooling of α -Al $\Delta T_n (= T_m - T_n)$ can be determined by DTA curves. ΔT_n for Al-2Cu alloy by adding 0.4% Al-5Ti-1B is 4.4 °C. It decreases further with La concentration less than 0.06% and then almost changes little with La addition. Figures 2–5 demonstrate that La and TiB_2 mainly affect nucleation process of α -Al, and the effect increases with La addition less than 0.06%. When more than 0.06% La is added, La-rich particles form and the effect of solute La left in matrix on the microstructure almost no longer changes.

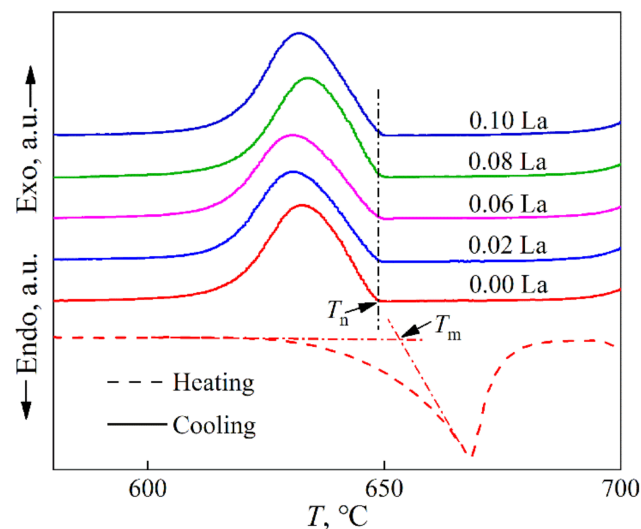


Figure 5. DTA heating and cooling curves for Al-2Cu alloy inoculated with 0.4% Al-5Ti-1B vs. La addition level. T_n and T_m are respectively the nucleation temperature and melting temperature. Heating/cooling rate is 10 K/min.

4. Discussion

As demonstrated in Figure 3, solutes La, Ti, and Cu segregate to Al(L)/TiB₂(S) interface. In the following discussion, we will first investigate the reason for solute segregation and then analyze its effect on grain refinement result of Al-5Ti-1B.

4.1. Segregation of La to Al Melt/TiB₂ Particles Interface along with Ti and Cu

For Al-2Cu alloy melt by adding La and Al-5Ti-1B, whether element *i* (*i* represents La, Ti, or Cu) enriches the melt/TiB₂ particles interface or not depends on the relationship between interfacial energies of pure solute *i*(L)/TiB₂(S) $\sigma_{i(L)/TiB_2(S)}^0$ and Al(L)/TiB₂(S) $\sigma_{Al(L)/TiB_2(S)}^0 = 0.853 \text{ J/m}^2$ and between the entropies of fusion of solute *i* ΔS_m^i and Al ΔS_m^{Al} , and the interaction energy parameters of solute *i* atom and Al atom in Al-*i* solution Ω_{Al-i} . $\sigma_{i(L)/TiB_2(S)}^0$ can be calculated by Equation (1) [25]:

$$\sigma_{i(L)/TiB_2(S)}^0 = \frac{0.364(2\Omega_{i-B} + \Omega_{i-Ti} - \Delta_f H_{TiB_2})}{3} + \frac{0.310f \cdot f_b^{1/3}(\Delta_m H_{Ti} + 2\Delta_m H_B)}{3} + (3.5 \pm 1)T \quad (1)$$

$$\omega_{i(L)/TiB_2(S)}$$

where $\Delta_f H_{TiB_2} = 323800 \text{ J/mol}$ is the heat of formation for TiB₂, $\Delta_m H_{Ti} = 14146 \text{ J/mol}$ and $\Delta_m H_B = 50200 \text{ J/mol}$ are respectively the enthalpies of fusion of Ti and B, $f_b = 0.74$ is the bulk packing factor, $f = 1.09$ [25], Ω_{i-B} and Ω_{i-Ti} are respectively the interaction energy parameters of *i*-B melt and *i*-Ti melt. $\omega_{i(L)/TiB_2(S)} \approx \sqrt{\omega_{i(L)}\omega_{Ti(L)}}$ is the molar area of *i*(L)/TiB₂(S) interface, $\omega_{i(L)} = f(N_a)^{1/3}V_{i(L)}^{2/3}$ is the molar area of *i* melt, $N_a = 6.02 \times 10^{23} \text{ mol}^{-1}$ is the Avogadro's number, $V_{La(L)} = 2.33 \times 10^{-5} \text{ m}^3/\text{mol}$, $V_{Ti(L)} = 1.16 \times 10^{-5} \text{ m}^3/\text{mol}$, and $V_{Cu(L)} = 7.94 \times 10^{-6} \text{ m}^3/\text{mol}$ are the molar volumes of La, Ti, and Cu melt, respectively [26].

Interaction energy parameter Ω_{j-i} (*j* represents Ti, B or Al, *j* ≠ *i*) is determined by Equation (2) [25]:

$$\Omega_{j-i}(1 - x_i)^2 = R_g T \ln \gamma_i \quad (2)$$

where γ_i is the activity coefficient of *i*, which is obtained by using Wilson equation $\ln \gamma_i = 1 - \ln(1 - x_j A_{j/i}) - x_i / (1 - x_j A_{j/i}) - x_j (1 - A_{i/j}) / (1 - x_i A_{i/j})$. $A_{i/j}$ and $A_{j/i}$ are the Wilson parameters [27].

Calculated results for $\sigma_{i(L)/TiB_2(S)}^0$ at 660 °C are shown in Figure 6. It is demonstrated that the values of $\sigma_{i(L)/TiB_2(S)}^0$ are less than $\sigma_{Al(L)/TiB_2(S)}^0$, indicating that solutes La and Cu tend to enrich Al(L)/TiB₂(S) interface along with solute Ti.

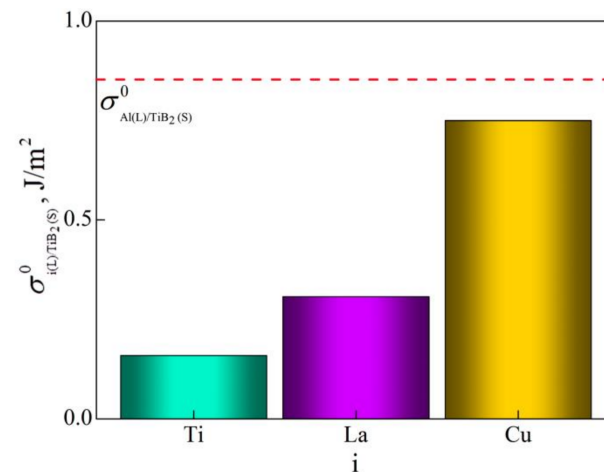


Figure 6. Interfacial energy $\sigma_{i(L)/TiB_2(S)}^0$ of *i*(L)/TiB₂(S) at 660 °C.

The mole fraction x_i^{In} of element i at Al(L)/TiB₂(S) interface depends on x_i^0 in the melt according to the following Equation (3) [25]:

$$\ln \left[\left(\frac{x_i^{In}}{1-x_i^{In}} \right) / \left(\frac{x_i^0}{1-x_i^0} \right) \right] = \frac{\frac{2\Omega_{Al-i}}{Z} [Z_L(x_i^{In}-x_i^0) - Z_1(x_i^0-0.5)] + (\Delta S_m^{Al} - \Delta S_m^i)T}{R_g T} - \frac{\omega_{i(L)/TiB_2(S)} (\gamma_{i(L)/TiB_2(S)}^0 - \gamma_{Al(L)/TiB_2(S)}^0)}{R_g T} \quad (3)$$

where $Z = 12$ and $Z_L = 6$ are respectively the atomic coordination numbers of the melt and interfacial monolayer; $Z_1 = 3$ is the atomic coordination number to one of the adjacent layers, $\Omega_{Al-Ti} = -120,000$ J/mol, ΔS_m^i and $\Delta S_m^{Al} = 11.47$ J/(mol·K) are respectively the entropies of fusion of i and Al ($\Delta S_m^{La} = 5.19$ J/(mol·K), $\Delta S_m^{Ti} = 7.288$ J/(mol·K) and $\Delta S_m^{Cu} = 9.768$ J/(mol·K) [25,28]).

Figure 7 shows the dependence of x_{La}^{In} on x_{La}^0 . It is demonstrated that x_{La}^{In} increases with x_{La}^0 and the variation of x_{La}^{In} with x_{La}^0 is almost unaffected by temperature especially for a low x_{La}^0 . Temperature effect on i segregation is thus reasonable to neglect.

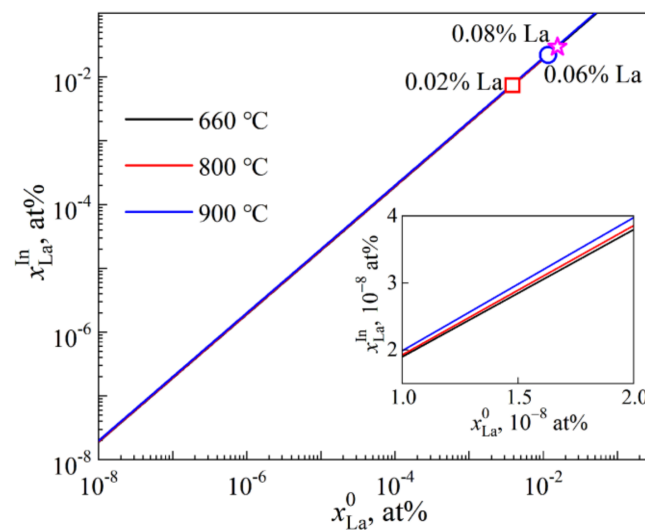


Figure 7. x_{La}^{In} as a function of x_{La}^0 . Symbols present the points corresponding to the La addition level to melt.

4.2. Effect of La and TiB₂ on Grain Refinement of Al-2Cu Alloy

Considering that nucleation and growth processes of α -Al determine microstructure evolution of Al-2Cu alloy. The synergetic effects of La and TiB₂ on grain refinement will be discussed from the above two aspects.

Restriction effect of i (i represents La or Cu) on the growth of α -Al grains can be calculated by Equation (4) [29]:

$$Q_i = \begin{cases} m_i c_i^0 (k_i - 1), & 0 < c_i^0 \leq c'_{iS} \\ \frac{m_i c_i^0 (k_i - 1) (c'_{iL} - c_i^0) k_i}{(c'_{iL} - c'_{iS}) - (1 - k_i) (c'_{iL} - c_i^0)}, & c'_{iS} < c_i^0 \leq c'_{iL} \end{cases} \quad (4)$$

where k_i and m_i are respectively the equilibrium partition coefficient and liquidus slope, c'_{iS} is the i solubility of primary α -Al and c'_{iL} is the eutectic composition.

According to Equation (4), $Q_{La}^{max}|_{0.05\%La} = 0.09$ K with $m_{La} = -1.71$ K/wt%, and $k_{La} = 0.004$ [30] is much less than $Q_{Ti} = 2.54$ K and $Q_{Cu} = 5.64$ K with $m_{Cu} = -3.4$ K/wt% and $k_{Cu} = 0.17$ [29], indicating that trace La effect on growth of α -Al grain is negligible. Thus, the addition of trace La and TiB₂ particles mainly affects the nucleation process of α -Al.

When α -Al nucleates homogeneously, nucleation rate I_{Hom} of α -Al is described (Equation (5)):

$$I_{\text{Hom}} = 10^{40} \exp\left(-\frac{16\pi\sigma_{\text{Al(L)}/\alpha\text{-Al(S)}}^3}{3k_{\text{b}}T_{\text{nHom}}\Delta G_{\text{VHom}}^2}\right) \quad (5)$$

where $\sigma_{\text{Al(L)}/\alpha\text{-Al(S)}} = 0.158 \text{ J/m}^2$ is the interfacial energy of Al(L)/ α -Al(S), $k_{\text{b}} = 1.38 \times 10^{-23} \text{ J/K}$ is the Boltzmann's constant, T_{nHom} is the homogeneous nucleation temperature, $\Delta G_{\text{VHom}} = \Delta S_{\text{V}}\Delta T_{\text{nHom}}$ is the driving force for homogeneous nucleation of α -Al with ΔT_{nHom} , and $\Delta S_{\text{V}} = 1.11 \times 10^6 \text{ J/(m}^3 \cdot \text{K)}$ [8] respectively being the homogeneous nucleation undercooling and entropy of fusion per unit volume.

When 0.4% Al-5Ti-1B and trace La are added to the melt, α -Al nucleates on the substrates, just like Ni-base superalloys [31]. Heterogeneous nucleation rate I_{Heter} of α -Al is as follows (Equation (6)):

$$I_{\text{Heter}} = 10^{40} \exp\left(-\frac{16\pi\sigma_{\text{Al(L)}/\alpha\text{-Al(S)}}^3}{3k_{\text{b}}T_{\text{nHeter}}\Delta G_{\text{VHeter}}^2}f(\theta)\right) \quad (6)$$

where T_{nHeter} is the heterogeneous nucleation temperature, $\Delta G_{\text{VHeter}} = \Delta S_{\text{V}}\Delta T_{\text{nHeter}}$ is the driving force for heterogeneous nucleation of α -Al with ΔT_{nHeter} being the heterogeneous nucleation undercooling, $f(\theta) = (\cos^3\theta - 3\cos\theta + 2)/4$ is the catalytic factor, θ the contact angle between α -Al and substrates.

When nucleation of α -Al just starts, it can be considered that $I_{\text{Hom}} = I_{\text{Heter}} = 10^6 \text{ m}^{-3} \text{ s}^{-1}$. $f(\theta)$ can be thus described as (Equation (7)):

$$f(\theta) = \frac{T_{\text{nHeter}}\Delta T_{\text{nHeter}}^2}{T_{\text{nHom}}\Delta T_{\text{nHom}}^2} \quad (7)$$

By using the relation $T_{\text{nHom}} = 1/3T_{\text{m}}$ [32], Equation (7) can be written as (Equation (8)):

$$f(\theta) = \frac{27(T_{\text{m}} - \Delta T_{\text{nHeter}})\Delta T_{\text{nHeter}}^2}{4T_{\text{m}}^3} \quad (8)$$

The contact angle θ can thus be determined according to the experimental conditions by using Equation (8), as shown in Figure 8. When trace La is added to melt, θ decreases and heterogeneous nucleation of α -Al occurs at a smaller undercooling. θ shows a tendency of first decrease with La addition below 0.06% and then almost being unchanged with La addition. Combined with Section 4.1, it can be concluded that heterogeneous nucleation potency of TiB₂ particles is enhanced by trace La addition due to solute segregation at Al(L)/TiB₂ interface. Grain refinement result of Al-5Ti-1B is thus improved by trace La addition.

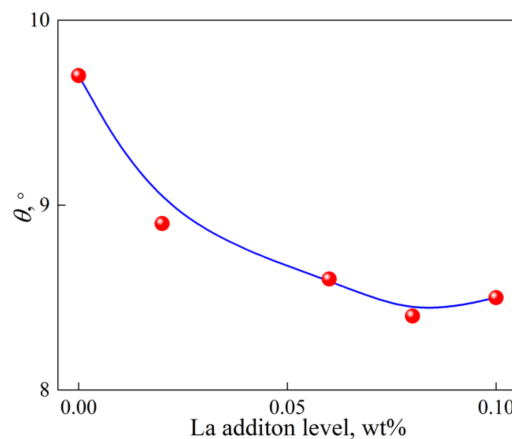


Figure 8. Calculated contact angle θ varied with trace La addition level.

5. Conclusions

- (1) Combinedly adding Al-5Ti-1B and trace La causes a further grain refinement result compared to the individual addition of Al-5Ti-1B. Average size of α -Al grains decreases first and then almost keeps unchanged with La addition. Satisfactory grain refinement result achieves when La addition reaches 600 ppm.
- (2) Theoretical calculations were carried out to investigate the segregation of solute La to melt/TiB₂ interface and segregation effect on grain refinement result of Al-5Ti-1B.
- (3) Synergistic effect of La and TiB₂ on grain refinement is mainly attributed to the enhancement in the heterogeneous nucleation potency of TiB₂ particles for α -Al by La segregation to Al melt/TiB₂ particles interface.

Author Contributions: Methodology, conceptualization, supervision, writing—review and editing, L.Z. and J.Z.; methodology and conceptualization, Y.S.; resources and visualization, L.Y., J.H. and H.J. All authors have read and agreed to the published version of the manuscript.

Funding: This research was funded by National Natural Science Foundation of China [Lili Zhang] grant number [51901231] and [Jiuzhou Zhao] grant number [51971227], National Key R&D Program of China [Jiuzhou Zhao] grant number [2021YFA0716303], and Natural Science Foundation of Liaoning Province [Lili Zhang] grant number [2019-BS-253].

Institutional Review Board Statement: Not applicable.

Informed Consent Statement: Not applicable.

Data Availability Statement: Data is contained within the article.

Conflicts of Interest: The authors declare no conflict of interest.

References

1. Queded, T.E. Understanding mechanisms of grain refinement of aluminum alloys by inoculation. *Mater. Sci. Technol.* **2013**, *20*, 1357–1369. [[CrossRef](#)]
2. Wang, Y.; Fang, C.M.; Zhou, L.; Hashimoto, T.; Zhou, X.; Ramasse, Q.M.; Fan, Z. Mechanism for Zr poisoning of Al-Ti-B based grain refiners. *Acta Mater.* **2019**, *164*, 428–439. [[CrossRef](#)]
3. Safyari, M.; Moshtaghi, M.; Hojo, T.; Akiyama, E. Mechanisms of hydrogen embrittlement in high-strength aluminum alloys containing coherent or incoherent dispersoids. *Corros. Sci.* **2022**, *194*, 109895. [[CrossRef](#)]
4. Maxwell, I.; Hellawell, A. A simple model for grain refinement during solidification. *Acta Metall.* **1975**, *23*, 229–237. [[CrossRef](#)]
5. Greer, A.L.; Bunn, A.M.; Tronche, A.; Evans, P.V.; Bristow, D.J. Modelling of inoculation of metallic melts: Application to grain refinement of aluminum by Al-Ti-B. *Acta Mater.* **2000**, *48*, 2823–2835. [[CrossRef](#)]
6. Easton, M.A.; Stjohn, D.H. A model of grain refinement incorporating alloy constitution and potency of heterogeneous nucleant particles. *Acta Mater.* **2001**, *49*, 1867–1878. [[CrossRef](#)]
7. Queded, T.E.; Greer, A.L. The effect of the size distribution of inoculant particles on as-cast grain size in aluminum alloys. *Acta Mater.* **2004**, *52*, 3859–3868. [[CrossRef](#)]
8. Queded, T.E.; Greer, A.L. Grain refinement of Al alloys: Mechanisms determining as-cast grain size in directional solidification. *Acta Mater.* **2005**, *53*, 4643–4653. [[CrossRef](#)]
9. Easton, M.A.; Stjohn, D.H. An analysis of the relationship between grain size, solute content, and the potency and number density of nucleant particles. *Metall. Mater. Trans. A* **2005**, *36*, 1911–1920. [[CrossRef](#)]
10. Easton, M.A.; Stjohn, D.H. Improved prediction of the grain size of aluminum alloys that includes the effect of cooling rate. *Mater. Sci. Eng. A* **2008**, *486*, 8–13. [[CrossRef](#)]
11. Qian, M.; Cao, P.; Easton, M.A.; McDonald, S.D.; Stjohn, D.H. An analytical model for constitutional supercooling-driven grain formation and grain size prediction. *Acta Mater.* **2010**, *58*, 3262–3270. [[CrossRef](#)]
12. Stjohn, D.H.; Qian, M.; Easton, M.A.; Cao, P. The interdependence theory: The relationship between grain formation and nucleant selection. *Acta Mater.* **2011**, *59*, 4907–4921. [[CrossRef](#)]
13. Prasad, A.; Yuan, L.; Lee, P.D.; Stjohn, D.H. The interdependence model of grain nucleation: A numerical analysis of the Nucleation-Free Zone. *Acta Mater.* **2013**, *61*, 5914–5927. [[CrossRef](#)]
14. Jiang, W.M.; Fan, Z.T.; Dai, Y.C.; Li, C. Effects of rare earth elements addition on microstructures, tensile properties and fractography of A357 alloy. *Mater. Sci. Eng. A* **2014**, *597*, 237–244. [[CrossRef](#)]
15. Pourbahari, B.; Emany, M. Effects of La intermetallics on the structure and tensile properties of thin section gravity die-cast A357 Al alloy. *Mater. Des.* **2016**, *94*, 111–120. [[CrossRef](#)]
16. Yi, H.; Zhang, D.; Sakata, T.; Mori, H. Microstructural evolution in as-cast hypereutectic Al-Si alloys with different La additions. *Z. Metallkd.* **2002**, *93*, 1237–1244. [[CrossRef](#)]

17. Nogita, K.; McDonald, S.D.; Dahle, A.K. Eutectic Modification of Al-Si Alloys with Rare Earth. *Met. Mater. Trans.* **2004**, *45*, 323–326. [[CrossRef](#)]
18. Tsai, Y.C.; Chou, C.Y.; Lee, S.L.; Lin, C.K.; Lin, J.C.; Lim, S.W. Effect of trace La addition on the microstructures and mechanical properties of A356(Al-7Si-0.35Mg) aluminum alloys. *J. Alloys Compd.* **2009**, *487*, 157–162. [[CrossRef](#)]
19. Chen, Y.; Pan, Y.; Lu, T.; Tao, S.; Wu, J. Effects of combinative addition of lanthanum and boron on grain refinement of Al-Si casting alloys. *Mater. Des.* **2014**, *64*, 423–426. [[CrossRef](#)]
20. Li, D.; Cui, C.; Wang, X.; Wang, Q.; Chen, C.; Liu, S. Microstructure evolution and enhanced mechanical properties of eutectic Al-Si die cast alloy by combined alloying Mg and La. *Mater. Des.* **2016**, *90*, 820–828. [[CrossRef](#)]
21. Qiu, C.; Miao, S.; Li, X.; Xia, X.; Ding, J.; Wang, Y.; Zhao, W. Synergistic effect of Sr and La on the microstructure and mechanical properties of A356.2 alloy. *Mater. Des.* **2017**, *114*, 563–571. [[CrossRef](#)]
22. Jiang, H.X.; Li, S.X.; Zheng, Q.J.; Zhang, L.L.; He, J.; Song, Y.; Deng, C.K.; Zhao, J.Z. Effect of minor lanthanum on the microstructures, tensile and electrical properties of Al-Fe alloys. *Mater. Des.* **2020**, *195*, 108991. [[CrossRef](#)]
23. Zhang, L.L.; Zheng, Q.J.; Jiang, H.X.; He, J.; Zhao, J.Z. Effect of La addition on microstructure evolution of hypoeutectic Al-6Si alloys. *J. Mater. Sci.* **2020**, *55*, 7546–7554. [[CrossRef](#)]
24. Zheng, Q.J.; Zhang, L.L.; Jiang, H.X.; Zhao, J.Z.; He, J. Effect mechanisms of micro-alloying element La on microstructure and mechanical properties of hypoeutectic Al-Si alloys. *J. Mater. Sci. Technol.* **2020**, *47*, 142–151. [[CrossRef](#)]
25. Zhang, L.L.; Zheng, Q.J.; Jiang, H.X.; Zhao, J.Z. Interfacial energy between Al melt and TiB₂ particles and efficiency of TiB₂ particles to nucleate α -Al. *Scr. Mater.* **2019**, *160*, 25–28. [[CrossRef](#)]
26. Iida, T.; Guthrie, R.I.L. *The Physical Properties of Liquid Metals*; Oxford University Press Inc.: New York, NY, USA, 1998.
27. Fan, T.; Yang, G.; Zhang, D. Thermodynamic effect of alloying addition on in-situ reinforced TiB₂/Al composites. *Metall. Mater. Trans. A* **2005**, *36*, 225–233. [[CrossRef](#)]
28. Barin, I. *Thermochemical Data of Pure Substances*, 3rd ed.; VCH Publishers: New York, NY, USA, 1995.
29. Zhang, L.L.; Jiang, H.X.; He, J.; Zhao, J.Z. A new model of growth restriction factor for hypoeutectic aluminum alloys. *Scr. Mater.* **2020**, *179*, 99–101. [[CrossRef](#)]
30. Elliott, R.P.; Shunk, F.A. The Al-La (Aluminum-Lanthanum) system. *Bull. Alloy Phase Diagr.* **1981**, *2*, 219–221. [[CrossRef](#)]
31. Tan, L.M.; Wang, G.M.; Guo, Y.; Fang, Q.H.; Liu, Z.C.; Xiao, X.Y.; He, W.Q.; Qin, Z.J.; Zhang, Y.; Liu, F.; et al. Additively manufactured oxide dispersion strengthened nickel-based superalloy with superior high temperature properties. *Virtual Phys. Prototyp.* **2020**, *15*, 555–569. [[CrossRef](#)]
32. Li, S.B.; Du, W.B.; Wang, X.D.; Liu, K.; Wang, Z.H. Effect of Zr Addition on the Grain Refinement Mechanism of Mg-Gd-Er Alloys. *Acta Metall. Sin.* **2018**, *54*, 911–917.